

Influence of Filled $d\pi$ -Manifold and L/L' Ligands on the Structure, Basicity, and Bond Rotations of the Octahedral and d^6 Amido Complexes $\text{TpRu}(L)(L')(\text{NHPH})$ ($\text{Tp} = \text{Hydridotris}(\text{pyrazolyl})\text{borate}$; $L = L' = \text{PMe}_3$ or $\text{P}(\text{OMe})_3$, or $L = \text{CO}$ and $L' = \text{PPh}_3$): Solid-State Structures of $[\text{TpRu}(\text{PMe}_3)_2(\text{NH}_2\text{Ph})][\text{OTf}]$, $[\text{TpRu}\{\text{P}(\text{OMe})_3\}_2(\text{NH}_2\text{Ph})][\text{OTf}]$, and $\text{TpRu}\{\text{P}(\text{OMe})_3\}_2(\text{NHPH})$

David Conner, K. N. Jayaprakash, T. Brent Gunnoe,* and Paul D. Boyle

Department of Chemistry, North Carolina State University, Raleigh, North Carolina 27695-8204

Received February 28, 2002

It has been suggested that the reactivity of π -donating ligands bound to late-transition-metal complexes is heightened due to high d-electron counts. Herein, the synthesis and characterization of the Ru(II) amine and Ru(II) amido complexes $[\text{TpRuL}_2(\text{NH}_2\text{Ph})][\text{OTf}]$ ($\text{OTf} = \text{trifluoromethanesulfonate}$) and $\text{TpRuL}_2(\text{NHPH})$ ($L = \text{PMe}_3$ or $\text{P}(\text{OMe})_3$) are presented, including solid-state X-ray diffraction studies of $[\text{TpRu}(\text{PMe}_3)_2(\text{NH}_2\text{Ph})][\text{OTf}]$, $[\text{TpRu}\{\text{P}(\text{OMe})_3\}_2(\text{NH}_2\text{Ph})][\text{OTf}]$, and $\text{TpRu}\{\text{P}(\text{OMe})_3\}_2(\text{NHPH})$. The pK_a 's of the Ru(II) amine complexes and the previously reported $[\text{TpRu}(\text{CO})(\text{PPh}_3)(\text{NH}_2\text{Ph})]^+$ have been estimated to be comparable to that of malononitrile in methylene chloride. In addition, the impact of the filled $d\pi$ -manifold (i.e., Ru(II) and d^6 octahedral systems) on barriers to rotation of the Ru–NHPH moieties has been studied. For $\text{TpRu}(\text{PMe}_3)_2(\text{NHPH})$ and $\text{TpRu}\{\text{P}(\text{OMe})_3\}_2(\text{NHPH})$, evidence for hindered rotation about the amido nitrogen and phenyl ipso carbon has been observed, and the relative N–C and Ru–N bond rotational barriers for the series of three amido complexes are discussed in terms of the π -conflict.

Introduction

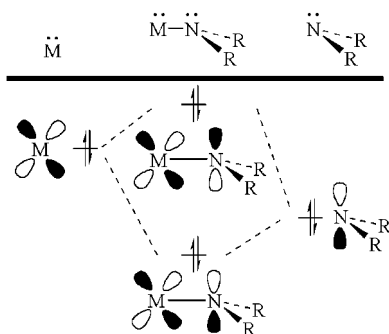
Late-transition-metal amido complexes are known to be important to a variety of important reactions.^{1–4} Since the homolytic bond strengths of late transition metal amido bonds have been demonstrated to be relatively strong,^{5,6} alternative explanations for the scarcity and high reactivity of such complexes have been proposed. For example, it has been suggested that the π -conflict between filled metal $d\pi$ -orbitals and ligand-based electron pairs is responsible, at least in part, for the paucity of late-transition-metal complexes with π -donating ligands.^{7,8} Along these lines, examples of octa-

hedral and d^6 amido complexes are relatively rare, and this is especially true for systems that lack aryl substituents on the amido ligand.^{5,6,9–21} Efforts directed toward the synthesis and reactivity of late transition metal amido complexes and

* Author to whom correspondence should be addressed. Fax: (919) 515-8909. E-mail: brent_gunnoe@ncsu.edu.

- (1) Hartwig, J. F. *Angew. Chem., Int. Ed.* **1998**, *37*, 2046–2067.
- (2) Roundhill, D. M. *Catal. Today* **1997**, *37*, 155–165.
- (3) Roundhill, D. M. *Chem. Rev.* **1992**, *92*, 1–27.
- (4) Müller, T. E.; Beller, M. *Chem. Rev.* **1998**, *98*, 675–703.
- (5) Bryndza, H. E.; Fong, L. K.; Paciello, R. A.; Tam, W.; Bercaw, J. E. *J. Am. Chem. Soc.* **1987**, *109*, 1444–1456.
- (6) Hartwig, J. F.; Andersen, R. A.; Bergman, R. G. *Organometallics* **1991**, *10*, 1875–1887.
- (7) Caulton, K. G. *New J. Chem.* **1994**, *18*, 25–41.
- (8) Mayer, J. M. *Comments Inorg. Chem.* **1988**, *8*, 125–135.

- (9) Kaplan, A. W.; Ritter, J. C. M.; Bergman, R. G. *J. Am. Chem. Soc.* **1998**, *120*, 6828–6829.
- (10) Fulton, J. R.; Bouwkamp, M. W.; Bergman, R. G. *J. Am. Chem. Soc.* **2000**, *122*, 8799–8800.
- (11) Hartwig, J. F.; Andersen, R. A.; Bergman, R. G. *J. Am. Chem. Soc.* **1989**, *111*, 2717–2719.
- (12) Macgregor, S. A.; MacQueen, D. *Inorg. Chem.* **1999**, *38*, 4868–4876.
- (13) Woerpel, K. A.; Bergman, R. G. *J. Am. Chem. Soc.* **1993**, *115*, 7888–7889.
- (14) Hsu, G. C.; Kosar, W. P.; Jones, W. D. *Organometallics* **1994**, *13*, 385–396.
- (15) Glueck, D. S.; Bergman, R. G. *Organometallics* **1991**, *10*, 1479–1486.
- (16) Glueck, D. S.; Winslow, L. J. N.; Bergman, R. G. *Organometallics* **1991**, *10*, 1462–1479.
- (17) Flood, T. C.; Lim, J. K.; Deming, M. A.; Keung, W. *Organometallics* **2000**, *19*, 1166–1174.
- (18) Dewey, M. A.; Arif, A. M.; Gladysz, J. A. *J. Chem. Soc., Chem. Commun.* **1991**, 712–714.
- (19) Dewey, M. A.; Knight, D. A.; Arif, A.; Gladysz, J. A. *Chem. Ber.* **1992**, *125*, 815–824.
- (20) Boncella, J. M.; Eve, T. M.; Rickman, B.; Abboud, K. A. *Polyhedron* **1998**, *17*, 725–736.

Scheme 1. The Presence of π -Conflict Leads to a Filled Antibond π^* -Molecular Orbital

related systems have begun to delineate the reactivity patterns of such complexes.^{22,23} According to the π -conflict theory, the reactive nature of high d-electron count complexes with π -donating ligands is derived from an occupied antibonding π^* -orbital (Scheme 1); however, the extent to which the π -conflict contributes to the reactivity of late transition metal amido complexes and the factors that control the π -conflict are not well understood.²⁴ Given the presence of late transition metal amido bonds in important reactions, understanding the features that modulate amido reactivity (and possibly the π -conflict) is important. Here, we report studies of $\text{TpRu}(\text{L})(\text{L}')(\text{NHPh})$ in which $\text{L} = \text{L}' = \text{PMe}_3$ or $\text{P}(\text{OMe})_3$, or $\text{L} = \text{CO}$ and $\text{L}' = \text{PPh}_3$, including the basicity of the amido ligands and the relative $\text{Ru}-\text{N}_{\text{amido}}$ and $\text{N}_{\text{amido}}-\text{C}_{\text{phenyl}}$ bond rotational barriers. To our knowledge, the $\text{TpRu}(\text{L})(\text{L}')(\text{NHR})$ ($\text{R} = \text{Ph}$ or H) systems are the first examples of a series of octahedral and d^6 amido complexes in which the ancillary ligands are varied.²⁵

Experimental Section

General Methods. All reactions and procedures were performed under anaerobic conditions in a nitrogen-filled glovebox or by using standard Schlenk techniques. Glovebox purity was maintained by periodic nitrogen purges and monitored by an oxygen analyzer (O_2 (g) < 15 ppm, for all reactions). Hexanes were purified by passage through a column of activated alumina.²⁶ THF, toluene, benzene, and diethyl ether were dried by distillation over sodium/benzophenone. Benzene- d_6 and CD_3CN were purified by distillation from CaH_2 , degassed, and stored over 4 Å sieves. CDCl_3 and CD_2Cl_2 were degassed via three freeze-pump-thaw cycles and stored over 4 Å sieves. ^1H and ^{13}C NMR spectra were obtained on a Varian Mercury 300 MHz or General Electric 300 MHz spectrometer. Resonances due to the Tp ligand are reported by chemical shift and multiplicity only. All $^3J_{\text{HH}}$ values for the pyrazolyl rings are 2 Hz. All ^1H and ^{13}C NMR spectra were referenced against tetramethylsilane using residual proton signals (^1H NMR) or the ^{13}C resonances of the deuterated solvent (^{13}C NMR). ^{31}P NMR spectra

were obtained on a Varian 300 MHz spectrometer and referenced against external 85% H_3PO_4 . All variable-temperature NMR experiments were performed on a General Electric 300 MHz spectrometer. UV-vis spectra were obtained on a Varian Cary 3E spectrophotometer. IR spectra were obtained on a Mattson Genesis II spectrometer either as thin films on a KBr plate or in a solution using a KBr solution plate. Electrochemical experiments were performed under a nitrogen atmosphere using a BAS Epsilon Potentiostat. Cyclic voltammograms were recorded in a standard three-electrode cell from -2.00 to $+2.00$ V with a glassy carbon working electrode and tetrabutylammonium hexafluorophosphate as an electrolyte. Tetrabutylammonium hexafluorophosphate was dried under a dynamic vacuum at 110 °C for 48 h prior to use. All potentials are reported versus NHE (normal hydrogen electrode) using cobaltocenium hexafluorophosphate as an internal standard. Elemental analyses were performed by Atlantic Microlabs, Inc. The syntheses of $\text{TpRu}(\text{CO})(\text{PPh}_3)(\text{NHPh})$ (**1**), $\text{TpRu}(\text{PMe}_3)_2(\text{OTf})$ (**2**), $\text{TpRu}\{\text{P}(\text{OMe})_3\}_2(\text{Cl})$ and $\text{TpRu}\{\text{P}(\text{OMe})_3\}_2(\text{OTf})$ (**3**) have been previously reported.^{25,27} $\text{Li}\{(\text{NC})_2\text{CH}\}$ was generated by the reaction of malononitrile with 1 equiv of $n\text{-BuLi}$ in benzene followed by vacuum filtration to collect the resulting white precipitate. All other reagents were used as purchased from commercial sources.

[TpRu(PMe₃)₂(NH₂Ph)](OTf) (4). $\text{TpRu}(\text{PMe}_3)_2(\text{OTf})$ (**2**) (1.3674 g, 2.222 mmol) was dissolved in approximately 50 mL of THF (OTf = trifluoromethanesulfonate). To this solution was added aniline (2.1295 g, 21.6 mmol), and the resulting mixture was allowed to stir for 24 h. The solution was concentrated to approximately 20 mL in vacuo, and diethyl ether (approximately 40 mL) was added to precipitate the product. The product was collected via vacuum filtration through a fine porosity frit and washed with diethyl ether (3×10 mL) to give a white solid (1.4089 g, 1.988 mmol, 90%). IR (thin film on KBr plate): $\nu_{\text{NH}} = 3285$ and 3262 cm^{-1} , $\nu_{\text{BH}} = 2481$ cm^{-1} . UV-vis (THF): $\lambda_{\text{max}} = 267$ nm ($\epsilon = 0.96 \times 10^4$ $\text{M}^{-1} \text{cm}^{-1}$). ^1H NMR (CD_3CN , δ): 7.85, 7.25 (each 2H, each a d, Tp CH 3 or 5 position), 7.80, 7.38 (each 1H, each a d, Tp CH 3 or 5 position), 6.95 (3H, m, overlap of $\text{NH}_2\text{C}_6\text{H}_5$ meta and para), 6.35 (2H, d, $^3J_{\text{HH}} = 7$ Hz, $\text{NH}_2\text{C}_6\text{H}_5$ ortho), 6.18 (2H, t, Tp CH 4 position), 6.14 (1H, t, Tp CH 4 position), 4.77 (2H, br s, NH_2Ph), 1.30 (18H, vt, $J_{\text{PH}} = 7$ Hz, $\text{P}(\text{CH}_3)_3$). $^{13}\text{C}\{^1\text{H}\}$ -NMR (CD_3CN , δ): 145.8, 142.7, 142.5, 136.9, 136.3 (each an s, Tp CH 3 or 5 position, and amine phenyl ipso carbon), 128.8, 125.1, 122.7 (each an s, amine phenyl ortho, meta, and para), 106.7, 106.0 (each an s, Tp CH 4 position), 18.1 (d, $^1J_{\text{PC}} = 12$ Hz). $^{31}\text{P}\{^1\text{H}\}$ -NMR (CDCl_3 , δ): 10.9. CV (THF, TBAH, 100 mV/s): $E_{\text{pa}} = 1.82$ V (Ru(III/II)). Anal. Calcd for $\text{C}_{22}\text{H}_{35}\text{BF}_3\text{N}_7\text{O}_3\text{P}_2\text{RuS}$: C, 37.29; H, 4.98; N, 13.84. Found: C, 37.16; H, 4.95; N, 13.61.

[TpRu{P(OMe)₃}₂(NH₂Ph)](OTf) (5). To a solution of $\text{TpRu}\{\text{P}(\text{OMe})_3\}_2(\text{Cl})$ (1.2587 g, 2.106 mmol) in approximately 50 mL of THF was added AgOTf (0.5413 g, 2.107 mmol). The resulting solution was refluxed for 20 h. During the reaction, the formation of a white precipitate (AgCl) was noted. The solution was cooled to room temperature and filtered through a fine porosity frit. Aniline (2.0564 g, 20.9 mmol) was added to the resulting solution. The mixture was allowed to stir for an additional 24 h. The solution was concentrated to approximately 20 mL in vacuo, and diethyl ether (approximately 40 mL) was added to precipitate the product. The product was collected via vacuum filtration through a fine porosity frit and washed with diethyl ether (3×10 mL) to give a white solid (1.5823 g, 1.967 mmol, 93%). IR (thin film on KBr plate): $\nu_{\text{NH}} = 3318$ and 3250 cm^{-1} , $\nu_{\text{BH}} = 2450$ cm^{-1} . UV-vis (THF): $\lambda_{\text{max}} = 223$ nm ($\epsilon = 2.0 \times 10^4$ $\text{M}^{-1} \text{cm}^{-1}$). ^1H NMR (CD_2 -

(21) Joslin, F. L.; Johnson, M. P.; Magee, J. T.; Roundhill, D. M. *Organometallics* **1991**, *10*, 2781–2794.

(22) Bryndza, H. E.; Tam, W. *Chem. Rev.* **1988**, *88*, 1163–1188.

(23) Fulton, J. R.; Holland, A. W.; Fox, D. J.; Bergman, R. G. *Acc. Chem. Res.* **2002**, *35*, 44–56.

(24) Holland, P. L.; Andersen, R. A.; Bergman, R. G. *Comments Inorg. Chem.* **1999**, *21*, 115–129.

(25) Jayaprakash, K. N.; Conner, D.; Gunnoe, T. B. *Organometallics* **2001**, *20*, 5254–5256.

(26) Pangborn, A. B.; Giardello, M. A.; Grubbs, R. H.; Rosen, R. K.; Timmers, F. J. *Organometallics* **1996**, *15*, 1518–1520.

(27) Jayaprakash, K. N.; Gunnoe, T. B.; Boyle, P. B. *Inorg. Chem.* **2001**, *40*, 6481–6486.

Cl₂, δ): 7.77, 7.39 (each 2H, each a d, Tp CH 3 or 5 position), 7.71, 7.63 (each 1H, each a d, Tp CH 3 or 5 position), 6.99 (3H, m, overlapping NH₂C₆H₅ meta and para), 6.35 (2H, d, ³J_{HH} = 7 Hz, NH₂C₆H₅ ortho), 6.16 (3H, m, overlapping Tp CH 4 position), 4.74 (2H, br s, NH₂C₆H₅), 3.44 (18H, vt, J_{PH} = 10 Hz, P(OCH₃)₃). ¹³C{¹H} NMR (CD₂Cl₂, δ): 148.3, 144.7, 137.7, 137.0 (each an s, Tp CH 3 or 5 position), 142.7 (amine phenyl ipso carbon), 129.9, 127.1, 124.7 (each an s, amine phenyl ortho, meta, and para), 106.8, 106.7 (each an s, Tp CH 4 position), 53.2 (br s, P(OCH₃)₃). ³¹P-{¹H} NMR (CD₃CN, δ): 139.3 (s, P(OCH₃)₃). CV (THF, TBAH, 100 mV/s): E_{p,a} = 1.86 V (Ru(III/II)). Anal. Calcd for C₂₂H₃₅-BF₃N₇O₉P₂RuS: C, 32.85; H, 4.39; N, 12.19. Found: C, 33.02; H, 4.28; N, 12.24.

TpRu(PMe₃)₂(NHPh) (6). A colorless solution of [TpRu(PMe₃)₂-NH₂Ph][OTf] (**4**) (0.1151 g, 0.162 mmol) in approximately 20 mL of THF was cooled to -78 °C. Sodium bis(trimethylsilyl)amide (0.178 mmol, 1.0 M in THF) was added dropwise via a microsyringe. After the addition of base, the color of the solution was noted to be pale yellow. The solution was allowed to warm to room temperature, and a color change to dark brown/yellow was noted. The volatiles were removed under reduced pressure. The resulting solid was dissolved in benzene (approximately 60 mL) and filtered through a fine porosity frit. Benzene was removed from the filtrate under reduced pressure to yield a pale yellow solid (0.082 g, 0.147 mmol, 90%). IR (solution cell in THF): ν_{NH} = 3326 cm⁻¹, ν_{BH} = 2467 cm⁻¹. UV-vis (THF): λ_{max} = 293 nm (ε = 1.7 × 10⁴ M⁻¹ cm⁻¹). ¹H NMR (C₆D₆, δ): 7.66, 7.47 (each 2H, each a d, Tp CH 3 or 5 position), 7.51, 6.89 (each 1H, each a d, Tp CH 3 or 5 position), 7.22 (2H, t, ³J_{HH} = 7 Hz, phenyl meta), 6.45 (1H, t, ³J_{HH} = 7 Hz, phenyl para), 5.88 (2H, t, Tp CH 4 position), 5.85 (1H, t, Tp CH 4 position), 2.80 (1H, br s, NHPh), 0.92 (18H, vt, J_{PH} = 6 Hz, P(CH₃)₃). At room temperature in C₆D₆, the resonances due to the ortho protons are broadened into the baseline. In CD₂Cl₂ at room temperature, the ortho protons are observed as a broad singlet at approximately 5.8 ppm. ¹³C{¹H} NMR (C₆D₆, δ): 163.3 (s, Ph ipso), 145.7, 142.8, 136.0, 135.8 (each an s, Tp CH 3 or 5 position), 129.4, 128.5, 115.9 (each an s, amido phenyl ortho, meta, and para), 106.0, 105.7 (each an s, Tp CH 4 position), 18.9 (d, ¹J_{PC} = 12 Hz, P(CH₃)₃). ³¹P{¹H} NMR (C₆D₆, δ): 17.5 (s, P(CH₃)₃). CV (THF, TBAH, 50 mV/s): E_{1/2} = -0.28 V (Ru(III/II)). Anal. Calcd for C₂₁H₃₁BN₇P₂Ru: C, 45.17; H, 6.14; N, 17.56. Found: C, 45.29; H, 6.17; N, 17.29.

TpRu{P(OMe)₃}₂(NHPh) (7). A colorless solution of [TpRu{P(OMe)₃}₂-NH₂Ph][OTf] (**5**) (0.1142 g, 0.142 mmol) in approximately 20 mL of THF was cooled to -78 °C. To this solution was added dropwise via a microsyringe sodium bis(trimethylsilyl)amide (0.156 mmol, 1.0 M in THF). After the addition of amide, the color of the solution was noted to be yellow. The solution was allowed to warm to room temperature, and a color change to dark yellow was noted. Removal of the volatiles under reduced pressure yielded a yellow solid. The resulting solid was dissolved in benzene (approximately 60 mL) and filtered through a fine porosity frit. Benzene was removed from the filtrate under reduced pressure to yield a bright yellow solid (0.085 g, 0.130 mmol, 91%). IR (solution cell in THF): ν_{NH} = 3378 cm⁻¹, ν_{BH} = 2467 cm⁻¹. UV-vis (THF): λ_{max} = 284 nm (ε = 1.3 × 10⁴ M⁻¹ cm⁻¹). ¹H NMR (C₆D₆, δ): 7.98, 7.56 (each 2H, each a d, Tp CH 3 or 5 position), 7.87, 7.46 (each 1H, each a d, Tp CH 3 or 5 position), 6.93 (2H, t, ³J_{HH} = 7 Hz, phenyl meta), 6.36 (1H, t, ³J_{HH} = 7 Hz, phenyl para), 6.00 (3H, m, overlap of Tp CH 4 position and phenyl ortho), 5.86 (1H, t, Tp CH 4 position), 3.14 (18H, vt, J_{PH} = 10 Hz, P(OCH₃)₃), 1.98 (1H, br s, NHPh). ¹³C{¹H} NMR (C₆D₆, δ): 163.3 (s, phenyl ipso), 145.7, 142.8, 136.0, 135.8 (each an s, Tp CH 3 or 5 position),

129.4, 128.5, 115.9 (each an s, amido phenyl ortho, meta, and para), 106.0, 105.7 (each an s, Tp CH 4 position), 18.9 (d, ¹J_{PC} = 12 Hz, P(OCH₃)₃). ³¹P{¹H} NMR (THF-*d*₈, δ): 137.5 (s, P(CH₃)₃). CV (THF, TBAH, 50 mV/s): E_{1/2} = -0.25 V (Ru(III/II)). Anal. Calcd for C₂₁H₃₄BN₇P₂O₆Ru-C₆H₆: C, 44.27; H, 5.50; N, 13.38. Found: C, 42.50; H, 5.42; N, 13.22.

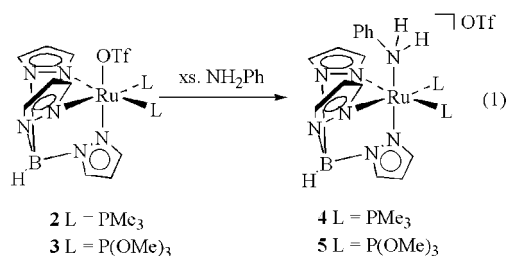
NMR Tube Reactions of Amido Complex 1, 6, or 7 with Malononitrile. All reactions followed the same general procedure. Inside a nitrogen-filled glovebox, an NMR tube was charged with a known amount of the appropriate amido complex. One equivalent of malononitrile was weighed out and dissolved in CD₂Cl₂, and this solution was added to the NMR tube with the amido complex. A ¹H NMR spectrum was immediately acquired at room temperature. Variable-temperature ¹H NMR experiments were performed by lowering the temperature of the NMR probe to -90 °C.

UV-Vis Experiments for Reactions of Amido Complex 6 or 7 with Malononitrile. The procedure that was utilized for the ¹H-NMR spectra of complexes **6** and **7** with malononitrile was followed. The reaction solutions were transferred to a quartz cuvette (sealed under nitrogen), and UV-vis spectra were acquired.

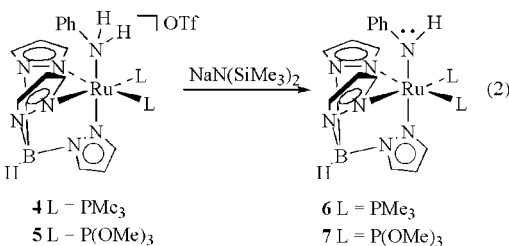
Crystal Structures of [TpRu(PMe₃)₂NH₂Ph][OTf] (4), [TpRu{P(OMe)₃}₂NH₂Ph][OTf] (5), and TpRu{P(OMe)₃}₂(NHPh) (7). For full details of X-ray structure determination of these complexes, please see Supporting Information.

Results

We have previously reported the synthesis of TpRu(CO)-(PPh₃)(NHPh) (**1**) as well as TpRu(PMe₃)₂(OTf) (**2**) and TpRu{P(OMe)₃}₂(OTf) (**3**) (OTf = trifluoromethanesulfonate).^{25,27} Ligand exchange of triflate upon reaction of **2** or **3** with excess aniline yields the corresponding Ru(II) amine complexes (eq 1). The amine complexes are charac-



terized by broad resonances for the amine protons at 4.77 and 4.74 ppm in the ¹H NMR spectra of **4** and **5**, respectively, and cyclic voltammetry experiments reveal irreversible oxidation waves at 1.82 and 1.86 V (versus NHE). The amine ligands of **4** and **5** are deprotonated upon treatment with NaN(SiMe₃)₂ to yield the amido complexes **6** and **7** (eq 2).



The amido protons for **6** and **7** resonate at 2.80 and 1.98 ppm, respectively, in their ¹H NMR spectra. The negative shifts for the Ru(III/II) oxidation potentials relative to the

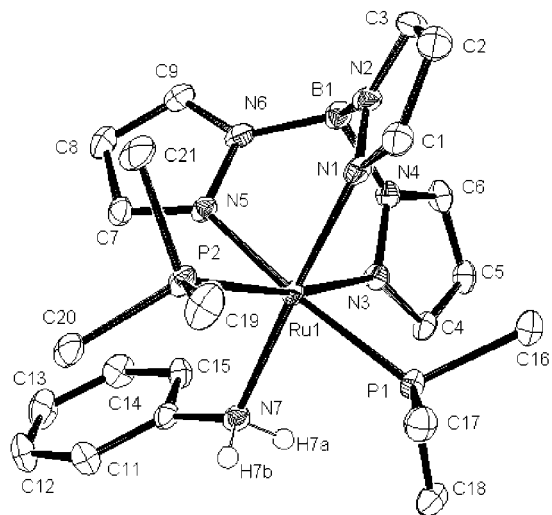


Figure 1. ORTEP diagram of [TpRu(PMe₃)₂(NH₂Ph)][OTf] (**4**).

Table 1. UV–Vis Data for Ru(II) Amine and Ru(II) Amido Complexes in THF

complex	λ_{\max} (nm)	ϵ (M ⁻¹ cm ⁻¹)
[TpRu(CO)(PPh ₃)(NH ₂ Ph)][OTf]	207	8.2×10^4
TpRu(CO)(PPh ₃)(NHPh) (1)	216	1.2×10^4
[TpRu(PMe ₃) ₂ (NH ₂ Ph)][OTf] (4)	267	0.96×10^4
[TpRu{P(OMe) ₃ } ₂ (NH ₂ Ph)][OTf] (5)	223	2.0×10^4
TpRu(PMe ₃) ₂ (NHPh) (6)	293	1.7×10^4
TpRu{P(OMe) ₃ } ₂ (NHPh) (7)	284	1.3×10^4

oxidation potentials of the amine complexes **4** and **5** ($E_{1/2} = -0.28$ and -0.25 V for **6** and **7**, respectively) are consistent with the deprotonation reactions. UV–vis data for the series of amine and amido complexes [TpRu(L)(L')(NH₂Ph)][OTf] and TpRu(L)(L')(NHPh) are shown in Table 1.

The X-ray structure of [TpRu(PMe₃)₂(NH₂Ph)][OTf] (**4**) shows a pseudooctahedral coordination sphere (Figure 1). Data collection parameters and selected bond distances and angles are displayed in Tables 2 and 3. The Ru–P bond distances are 2.3064(9) and 2.3116(10) Å. The Ru–N7–C10 bond angle is 123.6(2)°, and the N7–C10 bond distance is 1.444(5) Å. The N–C bond distance of aniline is 1.398 Å.²⁸ The Ru–N7 bond distance (2.211(3) Å) is slightly longer than the Ru–N bond distances of the Tp ligand (average Ru–N bond distance for the three pyrazolyl rings is 2.142(5) Å). The shorter Ru–N1 (Tp) bond distance (2.091(5) Å) compared with the other two Ru–pyrazolyl bond distances (average 2.167(4) Å) is indicative of an amine trans effect. Evidence of hydrogen bonding between the aniline ligand and triflate anion is observed in the structure of **4**. For example, bond distances between the amine protons and triflate oxygen atoms are 2.20(6) Å (H7(a)–O1) and 2.06(4) Å (H7(b)–O2), with N7–O1 and N7–O2 distances of 2.966(4) and 3.018(4) Å, respectively.

Inspection of the ORTEP diagram for [TpRu{P(OMe)₃}₂(NH₂Ph)][OTf] (**5**) indicates an amine orientation that is analogous to that of complex **4** (Figure 2). The Ru–phosphite bond distances of complex **5** are 2.2336(6) and 2.2209(6) Å. The Ru–N7–C10 bond angle (120.78(14)°) for the

Table 2. Selected Bond Distances (Å) and Angles (deg) for [TpRu(PMe₃)₂(NH₂Ph)][OTf] (**4**), [TpRu{P(OMe)₃}₂(NH₂Ph)][OTf] (**5**), and TpRu{P(OMe)₃}₂(NHPh) (**7**)

Bond Distances			
atoms	complex 4	complex 5	complex 7
Ru–P1	2.3064(9)	2.2336(6)	2.2275(5)
Ru–P2	2.3116(10)	2.2209(6)	2.2186(5)
Ru–N1	2.091(3)	2.0947(18)	2.1111(15)
Ru–N3	2.176(3)	2.1620(18)	2.1772(15)
Ru–N5	2.158(3)	2.1620(18)	2.1532(15)
Ru–N7	2.211(3)	2.1822(19)	2.1012(15)
N7–C10	1.444(5)	1.451(3)	1.365(2)
Bond Angles			
atoms	complex 4	complex 5	complex 7
P1–Ru–P2	100.79(3)	91.29(2)	92.822(17)
Ru1–N7–C10	123.6(2)	120.78(14)	135.30(13)
N7–C10–C11	120.5(3)	119.4(2)	120.50(16)
N7–C10–C15	119.6(3)	120.3(2)	115.84(16)
N1–Ru–N3	86.77(11)	87.57(7)	85.71(6)
N1–Ru–N5	88.65(11)	85.74(7)	86.24(6)
N3–Ru–N5	83.02(11)	83.96(7)	83.98(6)
N3–Ru–N7	90.51(11)	87.90(7)	92.45(6)
P1–Ru–N7	88.71(8)	86.81(5)	90.01(4)
P2–Ru–N7	95.79(9)	92.45(6)	89.52(4)
N1–Ru–N7	176.74(11)	175.43(7)	176.89(6)

Table 3. Selected Crystallographic Data and Collection Parameters for [TpRu(PMe₃)₂(NH₂Ph)][OTf] (**4**), [TpRu{P(OMe)₃}₂(NH₂Ph)][OTf] (**5**), and TpRu{P(OMe)₃}₂(NHPh) (**7**)

	complex 4	complex 5	complex 7
formula	C ₂₂ H ₃₄ BF ₃ –N ₇ O ₃ P ₂ RuS	C ₂₂ H ₃₅ BF ₃ –N ₇ O ₉ P ₂ RuS	C ₂₇ H ₄₀ B–N ₇ O ₆ P ₂ Ru
mol wt	707.43	804.43	732.48
cryst syst	triclinic	monoclinic	triclinic
space group	P1	P2 _{1/c}	P1
<i>a</i> , Å	9.4185(10)	9.1753(6)	9.8449(4)
<i>b</i> , Å	11.9282(14)	23.7851(18)	11.2687(4)
<i>c</i> , Å	14.0374(10)	15.3015(10)	14.8435(5)
α , deg	91.844(13)		86.667(3)
β , deg	93.045(13)	92.307(5)	87.380(4)
γ , deg	106.552(8)		87.854(4)
<i>V</i> , Å ³	1507.7(3)	3336.6(4)	1641.22(10)
<i>Z</i>	2	4	2
<i>D</i> _{calcd} , g cm ⁻³	1.558	1.601	1.482
total no.	5244	5817	5751
of reflns			
unique	5244	5817	5397
reflns			
<i>R</i>	0.028	0.025	0.022
<i>R</i> _w	0.045	0.030	0.038

phosphite complex is slightly reduced compared with that of complex **4**, and the N7–C10 bond distance (1.4531(3) Å) is close to that of complex **4**. The Ru–N7 bond distance (2.1822(19) Å) of complex **5** is shorter than that of complex **4** and is only slightly longer than the Ru–pyrazolyl bond distances (the average Ru–pyrazolyl bond distance is 2.139–(31) Å). As with complex **4**, the Ru–pyrazolyl–nitrogen bond distance trans to the amine ligand of complex **5** (2.0947(18) Å) is longer than the other two Ru–pyrazolyl bond distances (average bond distance of 2.1620(25) Å). Similar to complex **4**, hydrogen bonding is observed between the amine ligand and triflate anion (see Supporting Information for details).

The Ru–P bond distances (2.2275(5) and 2.2186(5) Å) of TpRu{P(OMe)₃}₂(NHPh) (**7**) are only slightly shorter than those of complex **5** (Figure 3). The Ru–N7 bond distance

(28) Fukuyo, M.; Hirotsu, K.; Higuchi, T. *Acta Crystallogr., Sect. B* **1982**, *38*, 640–643.

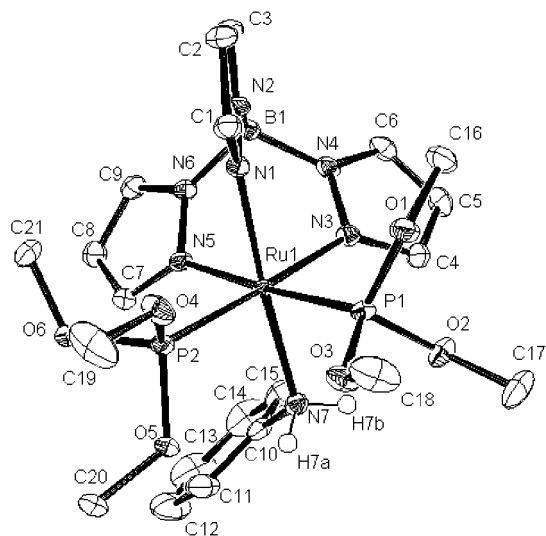
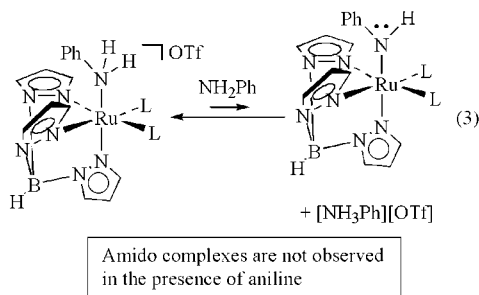


Figure 2. ORTEP diagram of $[\text{TpRu}\{\text{P}(\text{OMe})_3\}_2(\text{NH}_2\text{Ph})][\text{OTf}]$ (**5**).

of 2.1012(15) Å is almost identical to the Ru–N1 bond distance (2.1111(15) Å) of the *trans*-pyrazolyl ring. The average of the Ru–pyrazolyl bond distances is 2.1472(25) Å, and the Ru–N7–C10 bond angle is 135.30(13)°. The N7–C10 bond distance is 1.365(2) Å and is shorter than the analogous distance for the Ru(II) amine complexes **4** and **5**.

Recently, Bergman et al. have reported that the parent amido ligand of *trans*-(DMPE)₂Ru(H)(NH₂) (DMPE = 1,2-bis(dimethylphosphinoethane)) is highly basic,^{9,10} and we have reported similar observations for a series of TpRu(L)-(L')(NH₂) complexes.²⁵ Given the involvement of late transition metal amido complexes in catalytic reactions, the impact of a filled *dπ*-manifold on the reactivity of the amido ligands is of interest. The synthesis of the amine complexes $[\text{TpRu}(\text{PMe}_3)_2(\text{NH}_2\text{Ph})][\text{OTf}]$ (**4**) and $[\text{TpRu}\{\text{P}(\text{OMe})_3\}_2(\text{NH}_2\text{Ph})][\text{OTf}]$ (**5**) in the presence of excess aniline indicates that the free amine is not basic enough to deprotonate the metal-bound amine (eq 3).



This is in contrast to the octahedral and *d*⁴ tungsten complexes $[\text{Tp}^*\text{W}(\text{CO})(\text{PhC}_2\text{H})(\text{NH}_2\text{Ph})]^+$ and $[\text{Tp}^*\text{W}(\text{CO})_2(\text{NH}_2\text{Ph})]^+$ (Tp^* = hydridotris(3,5-dimethylpyrazolyl)borate) that are deprotonated to form amido complexes in the presence of excess aniline.^{29,30} The *pK*_a of PhNH₃⁺ is

(29) Powell, K. R.; Pérez, P. J.; Luan, L.; Feng, S. G.; White, P. S.; Brookhart, M.; Templeton, J. L. *Organometallics* **1994**, *13*, 1851–1864.

(30) Gunnoe, T. B.; White, P. S.; Templeton, J. L. *J. Am. Chem. Soc.* **1996**, *118*, 6916–6923.

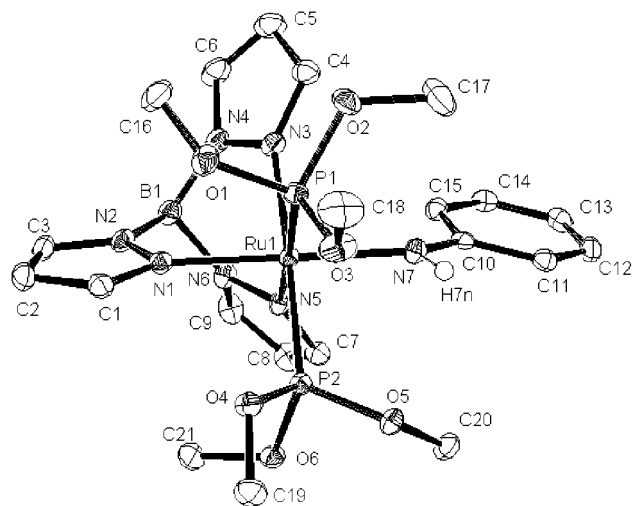
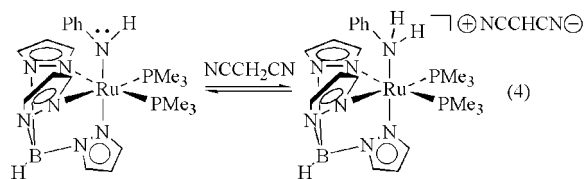


Figure 3. ORTEP diagram of $\text{TpRu}\{\text{P}(\text{OMe})_3\}_2(\text{NHPh})$ (**7**).

approximately 3.2 in dimethyl sulfoxide and is acidic enough to protonate the Ru(II) amido complexes $\text{TpRu}(\text{CO})(\text{PPh}_3)(\text{NHPh})$ (**1**), $\text{TpRu}(\text{PMe}_3)_2(\text{NHPh})$ (**2**), and $\text{TpRu}\{\text{P}(\text{OMe})_3\}_2(\text{NHPh})$ (**3**).³¹

To more accurately quantify the basicity of the three amido complexes $\text{TpRu}(\text{CO})(\text{PPh}_3)(\text{NHPh})$ (**1**), $\text{TpRu}(\text{PMe}_3)_2(\text{NHPh})$ (**6**), and $\text{TpRu}\{\text{P}(\text{OMe})_3\}_2(\text{NHPh})$ (**7**), we reacted each with weak acids. Dissolution of $\text{TpRu}(\text{CO})(\text{PPh}_3)(\text{NHPh})$ (**1**), $\text{TpRu}(\text{PMe}_3)_2(\text{NHPh})$ (**6**), or $\text{TpRu}\{\text{P}(\text{OMe})_3\}_2(\text{NHPh})$ (**7**) in CD₂Cl₂ with 1 equiv of methanol (*pK*_a = 16 in water) results in no observable reaction after 24 h. The ¹H NMR spectrum of a combination of $\text{TpRu}(\text{PMe}_3)_2(\text{NHPh})$ (**6**) with malononitrile in CD₂Cl₂ reveals an immediate reaction at room temperature. For example, the resonance due to the amido proton of **6** and the methylene protons of N≡CCH₂C≡N are not observed, and all other resonances are shifted relative to starting materials. In addition, broad resonances are observed at approximately 2.6 and 5.4 ppm. Addition of a second equivalent of malononitrile shifts the broad resonance at 2.6 ppm to 3.4 ppm. These results are consistent with the *rapid* equilibrium shown in eq 4, in which the broad resonances at 2.6 and 5.4 ppm are due to a four-site rapid proton exchange between the amido proton of **6**, the amine protons of $[\text{TpRu}(\text{PMe}_3)_2(\text{NH}_2\text{Ph})]^+$, the methylene protons of malononitrile, and the CH proton of the conjugate base of malononitrile (ion paired with the cationic amine complex).



At –90 °C the resonance at 2.6 ppm decoalesces, and new resonances (broad) are observed at 3.8 and 1.6 ppm. The resonances at 3.8 and 1.6 ppm are assigned to the CH₂ and CH protons of malononitrile and its conjugate base. Similar

(31) Isaacs, N. S. *Physical Organic Chemistry*; Wiley: New York, 1987.

results are observed with $\text{TpRu}(\text{CO})(\text{PPh}_3)(\text{NHPh})$ (**1**) and $\text{TpRu}\{\text{P}(\text{OMe})_3\}_2(\text{NHPh})$ (**7**). For example, the ^1H NMR spectrum of complex **1** with malononitrile -90°C shows broad resonances between 4.5 and 4.8 ppm (consistent with amido and amine proton chemical shifts), a broad resonance at approximately 3.8 ppm (malononitrile), and a broad resonance at 1.3 ppm (CH of malononitrile conjugate base). These four resonances coalesce at room temperature. The ^1H NMR spectrum of a 1/1 mixture of $\text{TpRu}\{\text{P}(\text{OMe})_3\}_2(\text{NHPh})$ (**7**) and malononitrile shows resonances consistent with a single TpRu complex (presumably the amine and amido complex in rapid equilibrium) and a broad resonance at approximately 2.4 ppm. The resonance at 2.4 ppm is assigned as the time average between the CH_2 group of malononitrile and the CH group of the malononitrile conjugate base. Addition of a second equivalent of malononitrile results in a shift of the resonance at 2.4 ppm to approximately 3.4 ppm.

To confirm that the amido complexes **6** and **7** are deprotonating malononitrile, UV-vis spectra of THF solutions of the amido complexes with malononitrile were acquired. The use of UV-vis spectroscopy to confirm an acid-base equilibrium of $\text{TpRu}(\text{CO})(\text{PPh}_3)(\text{NHPh})$ (**1**) and malononitrile was complicated by broad and overlapping absorptions for the amido complex **1** and the conjugate acid amine complex. The amido complex $\text{TpRu}(\text{PMe}_3)_2(\text{NHPh})$ (**6**) exhibits $\lambda_{\text{max}} = 293$ nm in its UV-vis spectrum, and the amine complex $[\text{TpRu}(\text{PMe}_3)_2(\text{NH}_2\text{Ph})][\text{OTf}]$ absorbs at $\lambda_{\text{max}} = 267$ nm. Neither malononitrile nor its lithiated anion absorb at $\lambda > 220$ nm. The UV-vis spectrum of a combination of complex **6** with 1 equiv of malononitrile shows an absorption at $\lambda_{\text{max}} \approx 267$ nm caused by the formation of the cationic amine (via deprotonation of malononitrile) with a red-shifted shoulder due to the amido complex **6** ($\lambda_{\text{max}} = 293$ nm). The combination of amido complex **7** with malononitrile exhibits similar results, and variation of malononitrile concentrations results in the observation of isosbestic points.

Due to the π -conflict, it was anticipated that the electronic contribution to the $\text{Ru}-\text{N}_{\text{amido}}$ bond rotation would be mitigated compared with systems in which the amido can efficiently π -donate into an empty metal $d\pi$ -orbital. In accord with this, the $\text{Ru}-\text{N}_{\text{amido}}$ rotational barrier for $\text{TpRu}(\text{CO})(\text{PPh}_3)(\text{NHPh})$ (**1**) was previously determined to be 12 kcal/mol (at -60°C),²⁷ and oxidation to $\text{Ru}(\text{IV})$ increases the barrier to rotation.³² For complex **1**, no evidence of restricted rotation around the $\text{N}_{\text{amido}}-\text{C}_{\text{phenyl}}$ bond is observed down to -100°C . In contrast, variable-temperature ^1H NMR for $\text{TpRu}(\text{PMe}_3)_2(\text{NHPh})$ (**6**) down to -100°C reveals no evidence for restricted rotation of the $\text{Ru}-\text{N}_{\text{amido}}$ bond. For example, no detectable changes are noted for the Tp, NH, PMe_3 , or the amido phenyl para proton resonances. At elevated temperatures, single resonances are observed for the ortho and meta protons of the amido phenyl. At reduced

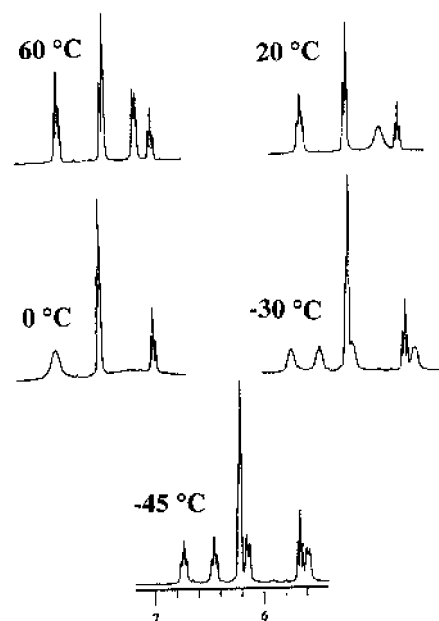


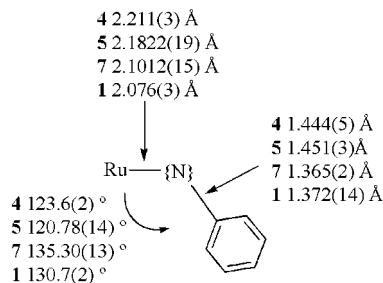
Figure 4. Variable-temperature ^1H NMR spectra of $\text{TpRu}(\text{PMe}_3)_2(\text{NHPh})$ (**6**) in the region from approximately 5.5 to 7.0 ppm in CD_2Cl_2 .

temperatures the ortho and meta resonances broaden and eventually decoalesce (Figure 4). These observations are consistent with hindered rotation around the amido nitrogen and ipso carbon of the phenyl ring, and the barrier at 0°C has been calculated to be 12.8 kcal/mol. The ^1H NMR spectrum of $\text{TpRu}\{\text{P}(\text{OMe})_3\}_2(\text{NHPh})$ (**7**) at 50°C reveals single resonances for the phenyl ortho and meta protons. At temperatures between 40 and -45°C these resonances broaden, decoalesce, and sharpen. In this temperature range there are no observed changes in the appearance of the Tp, NH, $\text{P}(\text{OMe})_3$, or phenyl para resonances. However, at -50°C the ortho and meta phenyl resonances begin to broaden again, and broadening of the resonances for the Tp, $\text{P}(\text{OMe})_3$, and phenyl para protons is also observed. The fluxional process at higher temperatures has been assigned as restricted rotation around the $\text{N}_{\text{amido}}-\text{C}_{\text{phenyl}}$ bond. Using the coalescence temperature (-20°C) for the ortho resonances, a lower limit for the $\text{N}-\text{C}$ rotational barrier was calculated to be 9.8 kcal/mol. Even though only a lower limit can be reported, no changes in the chemical shifts for the ortho resonances occur between -40 and -50°C (at which temperature line broadening due to the second process begins). Therefore, the calculated lower limit for the rotational barrier is most likely close in value to the actual barrier. In accord with the observations for $\text{TpRu}(\text{CO})(\text{PPh}_3)(\text{NHPh})$ (**1**), the second fluxional process has been assigned as hindered rotation about the $\text{Ru}-\text{N}$ bond; however, at -80°C the slow exchange region has not been established, and a barrier to rotation cannot be determined. Using Faller's guide for estimating free energies of activation according to the temperature at which line broadening begins, the $\text{Ru}-\text{N}$ bond rotational barrier complex **7** is likely to be <9.5 kcal/mol.³³

(32) Jayaprakash, K. N.; Gillespie, A. M.; Gunnoe, T. B.; White, D. P. *Chem. Commun.* **2002**, 4, 372–373.

(33) Faller, J. W. In *Encyclopedia of Inorganic Chemistry*; King, R. B., Ed.; Wiley: Chichester, U.K., 1994; Vol. 7, pp 3914–3933.

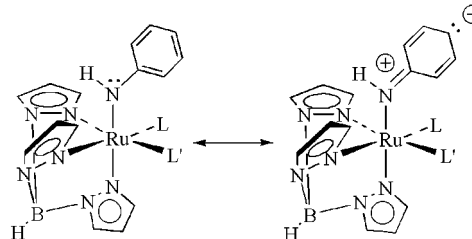
Chart 1. Variation of Bond Distances and Angles for Complexes **1**, **4**, **5**, and **7** ($\{N\} = \text{NH}_2$ for Complexes **4** and **5** and NH for Complexes **1** and **7**)



Discussion

We have previously discussed an inverse correlation between $\text{Ru}-\text{N}_{\text{amido}}$ and $\text{N}_{\text{amido}}-\text{C}_{\text{phenyl}}$ bond distances for a series of three Ru(II) phenyl amido complexes, and the trend was suggested to reflect the extent of electron density at the d^6 metal center.²⁷ That is, as the electron density at the metal center is increased the delocalization of the amido lone pair into the phenyl π^* system is increased (resulting in shorter $\text{N}_{\text{amido}}-\text{C}_{\text{phenyl}}$ bond distances). The $\text{Ru}-\text{N}_{\text{amido}}$ and $\text{N}_{\text{amido}}-\text{C}_{\text{phenyl}}$ bond distances of the amido complexes **7** and **1** are consistent with previous observations, although the difference in $\text{N}_{\text{amido}}-\text{C}_{\text{phenyl}}$ bond distances between **7** and **1** is not dramatically pronounced. As shown in Chart 1, there is a substantial difference in $\text{Ru}-\text{N}$ and $\text{N}_{\text{amido}}-\text{C}_{\text{phenyl}}$ bond distances upon deprotonation of the amine complex to yield the amido complex $\text{TpRu}\{\text{P}(\text{OMe})_3\}_2(\text{NHPh})$ (**7**). The amine complex $[\text{TpOs}(\text{NH}_2\text{Ph})\text{Cl}_2][\text{OTf}]$ has a $\text{p}K_a$ of approximately 3 in acetonitrile which corresponds to an acidity that is approximately 8 orders of magnitude greater than that of NH_3Ph^+ in acetonitrile.³⁴ Ruthenium(III) hexaammine has been reported to have a $\text{p}K_a$ of approximately 13.1 in aqueous solution.³⁵ The $\text{p}K_a$'s of the amine complexes $[\text{TpRu}(\text{L})(\text{L}')(\text{NH}_2\text{Ph})]^+$ are similar to that of malononitrile in methylene chloride. The $\text{p}K_a$ of malononitrile in THF has been reported to be 12.0;³⁶ however, this value has recently been brought into question.³⁷ In comparison with Mayer's $\text{TpOs}(\text{NHPh})\text{Cl}_2$ complex ($\text{p}K_a \approx 3$ for the corresponding amine), the filled $d\pi$ -orbitals of the Ru(II) amido complexes reported herein increase amido basicity by several orders of magnitude (the identity of the metal center and ancillary ligands may also have an impact). In addition, the presence of an amido phenyl substituent decreases the basicity by several orders of magnitude relative to the corresponding parent amido complexes.²⁵ The fact that the Ru(II) amine complexes are not deprotonated by aniline suggests that coordination to the Ru(II) metal increases the amine acidity to a lesser extent relative to the "binding" of the amine by a proton. That is, the amido ligands of the $\text{TpRu}(\text{L})(\text{L}')(\text{NHPh})$ complexes are more basic than aniline. Whether the difference in acidity

Scheme 2. Resonance Structures Resulting in $\text{N}_{\text{amido}}-\text{C}_{\text{ipso}}$ Multiple Bond Character for the Ru(II) Amido Complexes $\text{TpRu}(\text{L})(\text{L}')(\text{NHPh})$



between Ru(II)- NH_2Ph cations and NH_3Ph^+ is due to π -effects of the Ru(II) amido systems or to differences in bond polarization is difficult to discern. The electronegativity differences between a hydrogen atom and a ruthenium atom are significant; however, the results with $\text{TpOs}(\text{NHPh})\text{Cl}_2$ suggest that π -effects may play a role in substantially increasing the acidity of metal-bound amine ligands by stabilizing the resulting amido ligands via π -donation.

The small barrier to rotation about the $\text{Ru}-\text{N}_{\text{amido}}$ bond (12 kcal/mol) of $\text{TpRu}(\text{CO})(\text{PPh}_3)(\text{NHPh})$ has been attributed to the lack of π -interaction between the amido ligand and metal center, and it has been suggested that the sterically bulky Tp and PPh_3 ligands contribute significantly to the 12 kcal/mol barrier.²⁷ Interestingly, the $\text{TpRu}(\text{PMe}_3)_2(\text{NHPh})$ (**6**) complex shows no evidence of restricted rotation around the $\text{Ru}-\text{N}_{\text{amido}}$ bond down to -100 °C. This result could be due to either a small barrier to $\text{Ru}-\text{N}_{\text{amido}}$ bond rotation or the thermodynamic preference for a single isomer. For complex **6**, restricted rotation about the $\text{N}_{\text{amido}}-\text{C}_{\text{phenyl}}$ bond is observed, and the restricted N—C bond rotation can be attributed to the delocalization of the amido lone pair into the phenyl π^* system (Scheme 2). Structural data of $\text{TpRu}\{\text{P}(\text{OMe})_3\}_2(\text{NHPh})$ (**7**) and the corresponding amine complex $[\text{TpRu}\{\text{P}(\text{OMe})_3\}_2(\text{NH}_2\text{Ph})][\text{OTf}]$ (**5**) support the contribution of the resonance structure with $\text{N}=\text{C}$ character. The $\text{N}_{\text{amido}}-\text{C}_{\text{phenyl}}$ bond distance is shorter by 0.086(4) Å for **7** than for complex **5**. In addition, the C10—C15 bond distance of complex **7** is longer than that of complex **5** by 0.035(5) Å. The chemical shifts of the phenyl amido resonances also indicate that the amido electron density is being delocalized into the π^* -system. For example, the resonances due to the para proton and one of the ortho protons of $\text{TpRu}(\text{PMe}_3)_2(\text{NHPh})$ (**6**) are upfield of 6.0 ppm. In contrast, the resonances for the phenyl ring of $[\text{TpRu}(\text{PMe}_3)_2(\text{NH}_2\text{Ph})][\text{OTf}]$ are downfield of 6.0 ppm. Halide-substituted phenyl amido systems of Pt(II) have been reported to have N—C rotational barriers of 10.2–13.5 kcal/mol, and Hillhouse et al. have reported a N—C bond rotational barrier of 11.7 kcal/mol for $(\text{bpy})\text{Ni}(\text{Et})\text{N}(\text{tolyl})(\text{Et})$.^{38,39} Similarly, the phosphite complex $\text{TpRu}\{\text{P}(\text{OMe})_3\}_2(\text{NHPh})$ (**7**) exhibits a barrier to rotation about the $\text{N}_{\text{amido}}-\text{C}_{\text{phenyl}}$ bond of approximately 9.8 kcal/mol (lower limit), and although the slow exchange region cannot be accessed, evidence of restricted Ru—N bond rotation is observed at lower temperatures. Since the slow exchange

(34) Soper, J. D.; Bennett, B. K.; Lovell, S.; Mayer, J. M. *Inorg. Chem.* **2001**, *40*, 1888–1893.

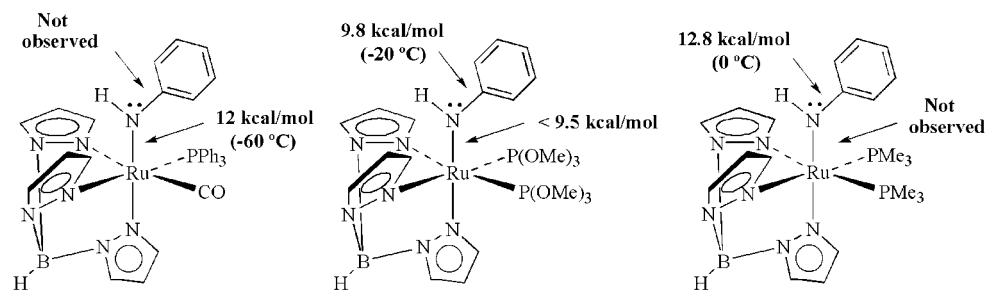
(35) Waysbort, D.; Navon, G. *Inorg. Chem.* **1979**, *18*, 9–13.

(36) Antipin, I. S.; Gareyev, R. F.; Vedernikov, A. N.; Kononov, A. I. *J. Phys. Org. Chem.* **1994**, *7*, 181–191.

(37) Abdur-Rashid, K.; Fong, T. P.; Greaves, B.; Gusev, D. G.; Hinman, J. G.; Landau, S. E.; Lough, A. J.; Morris, R. J. *J. Am. Chem. Soc.* **2000**, *122*, 9155–9171.

(38) Albéniz, A. C.; Calle, V.; Espinet, P.; Gómez, S. *Inorg. Chem.* **2001**, *40*, 4211–4216.

(39) Matsunaga, P. T.; Hess, C. R.; Hillhouse, G. L. *J. Am. Chem. Soc.* **1994**, *116*, 3665–3666.

Scheme 3. Relative Barriers to Bond Rotation for a Series of Ru(II) Amido Complexes

region has not been accessed for this process, we are not able to definitively assign it as Ru–N restricted rotation. However, in analogy to complex **1** and related systems, hindered Ru–N rotation is the most feasible explanation.^{19,27} These results highlight an apparent trend for the activation barriers to bond rotation about the three $N_{\text{amido}}-C_{\text{phenyl}}$ bonds. That is, the most electron-donating ligand set (i.e., complex **6**) exhibits the greatest barrier to rotation (12.8 kcal/mol); the rotational barrier for complex **7** is intermediate, and that of complex **1** is smallest ($6 > 7 > 1$). The observed trend suggests that increased π -conflict *may* influence the extent of delocalization of the amido lone pair into the phenyl π^* -system. In contrast, the expected trend due to steric factors would give a decreasing barrier to rotation in the order $1 > 6 > 7$. In addition, we note that the Ru–N rotational barrier is *apparently* greater for complex **1** than for complexes **6** and **7** (Scheme 3). This is consistent with the possibility of a three-center orbital interaction between the amido ligand, Ru, and CO leading to some multiple bonding between the amido ligand and metal center. In such a scenario, the decreased Ru–N bond rotational barriers for complexes **6** and **7** would be attributed to a combination of increased metal electron density (i.e., a more-donating ligand set) and nearly degenerate orthogonal metal $d\pi$ -orbitals. However, the presence of the bulky PPh_3 ligand also suggests that steric factors may make a significant contribution to the rotational barrier. As previously reported, the solid-state structure of **1** provides little evidence for a three-center interaction. Therefore, the tentative conclusion is that the increased Ru–N rotational barrier for complex **1** compared with complexes

6 and **7** is due primarily to differences in the steric contributions of the L and L' ligands, and that π -interactions play a minor role in the barrier to Ru– N_{amido} bond rotation. In contrast, the electronic nature of the metal center seemingly plays an important role in the N–C bond rotational barrier.

Summary

The basicity of a series of octahedral and d^6 phenyl amido complexes with variable ligand sets has been studied, and the $\text{p}K_{\text{a}}$'s of the conjugate acid aniline complexes have been estimated to be similar to that of malononitrile. The low acidity of the cationic aniline systems is attributed to the filled $d\pi$ -manifold of the metal center. In addition, the impact of the filled $d\pi$ -orbitals is observed in the variation of Ru– N_{amido} and $N_{\text{amido}}-C_{\text{phenyl}}$ bond rotational barriers as well as solid-state geometric features.

Acknowledgment. Acknowledgment is made to the donors of the Petroleum Research Fund (administered by the American Chemical Society) and to North Carolina State University for support of this research. We thank Mr. Roger Sullivan and the Martin research group (NCSU Department of Chemistry) for use of the UV–vis spectrophotometer.

Supporting Information Available: Complete tables of crystal data, collection and refinement data, atomic coordinates, bond distances and angles, and anisotropic displacement coefficients for **4**, **5**, and **7**. This material is available free of charge via the Internet at <http://pubs.acs.org>.

IC020163J